INTERNATIONAL JOURNAL OF HYDROGEN ENERGY 42 (2017) 6455–6461

Available online at www.sciencedirect.com

ScienceDirect

journal homepage: www.elsevier.com/locate/he

The noble metal loading binary iron–zinc electrode for hydrogen production

Murat Farsak [a,*], Esra Telli [b], Ayşe Ongun Yüce [c], Gülfeza Kardaş [c]

[a] Osmaniye Korkut Ata University, Science and Letter Faculty, Chemistry Department, Turkey
[b] Osmaniye Korkut Ata University, Engineering Faculty, Energy Systems Engineering Faculty, Turkey
[c] Çukurova University, Science and Letter Faculty, Chemistry Department, Turkey

ARTICLE INFO

Article history:
Received 4 October 2016
Received in revised form
10 November 2016
Accepted 11 November 2016
Available online 30 November 2016

Keywords:
Hydrogen production
Binary electrode
Cathode material
Electrodeposition

ABSTRACT

The binary FeZn was electrodeposited on graphite surface for hydrogen evolution reactions. Then, zinc was leached from the surface by an etching method in alkaline solution. A trace amount of platinum and ruthenium electrochemically deposited on binary FeZn, respectively. All electrodes were characterized by cyclic voltammetry, electrochemical impedance spectroscopy and potentiodynamic polarization techniques in KOH solution. The surface structures were characterized by scanning electron microscopy and energy dispersive X-ray. The results show that etching process enhanced the surface area. The prepared electrodes exhibited much higher activity after noble metal loadings. It is seen from experimental research that the most active electrode is C@FeZn/Ru.

Introduction

Hydrogen evolution reaction (HER) is one of the most popular topics because of the needs of clean, renewable energy at the recent time [1–5]. The development of new and efficient electrocatalysts for HER is vital to produce hydrogen which is clean energy carrier and promising as environmentally. HER is critical due to its use in technological areas such as fuel cells, chloro-alkaline industry, the photolytic and electrolytic water electrolyze. Therefore, the process is one of the most investigated reaction [6–10].

The cathodic electrocatalysts, which are effective and durable materials, are used as catalysts for HER [11]. Preferring the cheaper electrode materials, which have low overvoltage at high current density and in stable against highly corrosive electrolyte cells, is crucial to bring down the cost of electrolysis of water [12,13]. Low costly supporting electrodes and electrocatalytic materials having improved activity can reduce the cost of hydrogen production.

Carbon is used as supporting materials for many years, in preparing the different catalytical processes such as metal catalyst, activated carbon, carbon black, graphite and graphitic materials [14]. Fe, Ni, Co and their alloys are noteworthy as the electrocatalyst for HER due to their relatively low price and high accessibility by comparison with noble metals [15–18].

There are various methods of electrocatalyst production. The electrodeposition is the most preferred technique due to simplicity, low cost and the possibility to influence easily on the structure, composition, and properties of deposits obtained [11,19]. Iron and its compounds are significantly

* *Corresponding author*. Fax: +90 328 825 0097.
E-mail address: muratfarsak@osmaniye.edu.tr (M. Farsak).
http://dx.doi.org/10.1016/j.ijhydene.2016.11.078

remarkable as iron-based electrocatalyst because of their low price, readily available and low-toxic materials.

The catalytic activity of the electrode material can be developed either increasing ratio between the real and geometric surface area or changing the synergistic combination of the electrocatalytic component. The roughness of enhanced surface raises the contact area of electrolyte/electrocatalyst thereby electrochemically active surface area increases [20]. The etching process to zinc base alloys is widely used in the literature. The catalyst becomes a porous structure via this etching process. Moreover, the catalyst obtained which has high catalytic activity and large surface area [17,21–23].

Despite the noble metals such as Pt, Ru have high catalytic activity, but it is not preferred to use directly in industrial applications due to their high cost [24]. Therefore, lower amounts of noble metals are used in the development of high-performance electrodes with low noble metal loading. In this way, while reducing the amount of noble metal, activity increases significantly [25–28].

The study is aimed to occur new metallic alloys (FeZn, FeZn/Pt, and FeZn/Ru) having different matrixes for HER in alkaline electrolyte. Therefore, FeZn/Ru was selected for this purpose in this study.

Experimental

The working electrodes were prepared by using cylindrical graphite rod about 5 cm length. Graphite rod was drilled from the topside and copper wire put in the hole to provide the conductivity. The graphite rod immersed in the polyester mixture except for one side which has 0.283 cm^2 surface area. The open surface was abraded with emery papers (320–1200 grain size) before each experiment. Then the electrode surface was rinsed double distilled water, ethanol, and distilled water, respectively. The electrodeposition was performed galvanostatically using potentiostat-galvanostat (Gamry Interface 1000) by using the three-electrode technique. Ag/AgCl and Pt were used as a reference and counter electrodes, respectively.

The electrodeposition of the iron–zinc coating was performed galvanostatically using a direct current power supply instrument (TT Technic-YH-303D). The counter electrode was the platinum sheet, which has a 2 cm^2 surface area. The electrodes were coated with a bath solution mixed at a constant speed at room temperature. Coating thickness was calculated approximately by Faraday's laws. Iron-zinc was coated on the graphite surface by a constant current density of 15 mA cm^{-2} to the electrolysis system during 2700 s.

The electrodes were treated with 1 M NaOH for an hour and 30% NaOH for 2 h at room temperature, respectively. 1 M NaOH decreased the dissolution rate of Zn. 30% NaOH leached the Zn producing a porous electrode of high surface area. The electrode was washed with double distilled water.

The electrochemical characterizations of electrodes were analyzed by electrochemical impedance spectroscopy (EIS), cyclic voltammetry (CV) and potentiodynamic polarization techniques. EIS experiments were done by a range of frequency from 10^6 to 0.01 Hz at 5 mV amplitude. CV curves were obtained at 100 mV s^{-1} scan rate. Moreover, the potentiodynamic polarization plots were measured from open circuit potential to cathodic direction with 1 mV s^{-1} scan rate. All of the experiments were done in 1.00 M KOH solution at room temperature.

1 mg cm^{-2} Ru or Pt was deposited on the leached C/FeZn electrode by 15 mA cm^{-2}. The electrode was washed with distilled water and used for further electrochemical measurements. All of the bath compositions were given in Table 1. Fig. 1 shows the flow chart for the electrode preparation.

Table 1 – Bath compositions.

	Bath composition	Time (s)
Fe–Zn	30.86 g $FeSO_4 \cdot 7H_2O$, 31.92 g $ZnSO_4 \cdot 7H_2O$ and 1.2 g H_3BO_3	2700
Pt	2.49 mg Pt + 0.1 M KCl (50 mL volume)	70
Ru	2.05 mg Ru + 0.1 M KCl (50 mL volume)	203

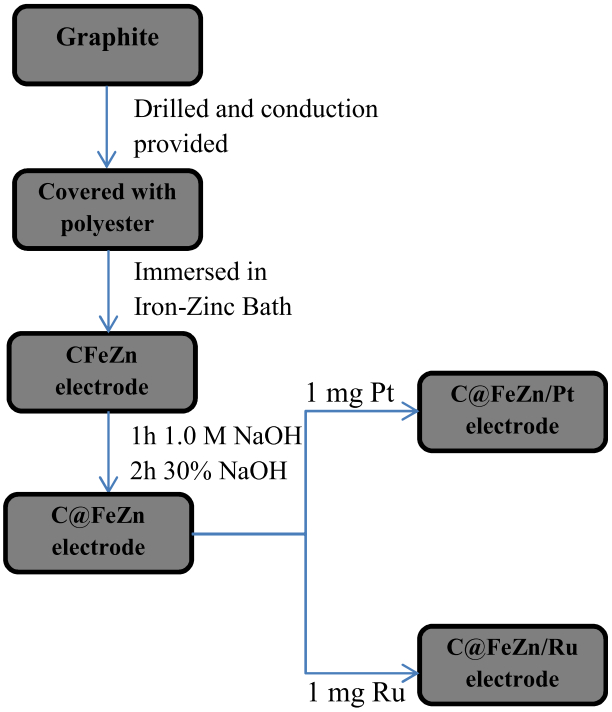

Fig. 1 – The flow chart for electrode preparation.

Results and discussion

The CV results of CFeZn (not etching), C@FeZn C@FeZn/Pt, C@FeZn/Ru (@ is etching symbol) electrodes in 1.0 M KOH solution at room temperature are illustrated in Fig. 2. When the alkaline leached Zn from the electrode surfaces, the peaks of C@FeZn electrode is larger and wider. Therefore, we have continued by etching after all electrodes were coated. The differences in the catalytic behavior of electrodes are shown in Fig. 2. As seen in Fig. 2, the peaks about −1.20 $V_{Ag/AgCl}$, −0.86 $V_{Ag/AgCl}$ and 0.66 $V_{Ag/AgCl}$ belong to Fe/Fe^{++}, Zn/Zn^{++} and

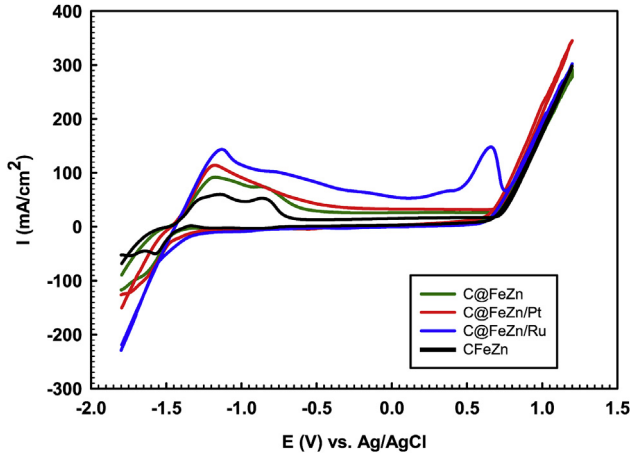

Fig. 2 – The cyclic voltammograms of CFeZn, C@FeZn, C@FeZn/Pt, C@FeZn/Ru electrodes at room temperature in 1.0 M KOH electrolyte at 100 mV s^{-1} scan rate.

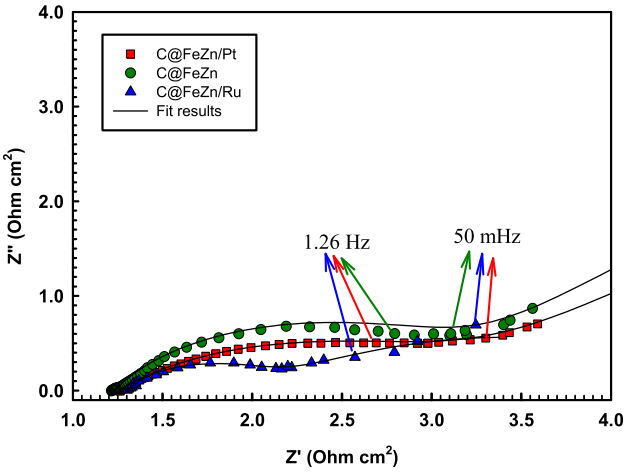

Fig. 3 – The Nyquist plots of C@FeZn, C@FeZn/Pt and C@FeZn/Ru electrodes in 1.0 M KOH.

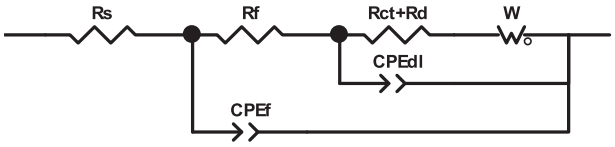

Fig. 4 – The equivalent circuit diagram for electrode/solution interface in 1.0 M KOH solution.

Ru^{++}/Ru^{+6} oxidations at anodic direction, respectively [14,29]. After noble metal loading, Zn effect is dominated because surface covered by noble metals. However, a faint peak belongs to Zn/Zn^{++} was seen after Ru loading due to completely uncovered surface. The hydrogen evolution overpotentials of prepared catalysts were measured as −1.262, −1.220, −1.210 and −1.200 V (vs. Ag/AgCl) for CFeZn, C@FeZn C@FeZn/Pt, C@FeZn/Ru electrodes, respectively.

Fig. 2 also shows the hydrogen evolution overpotentials of the catalysts. The overpotential of CFeZn, C@FeZn, C@FeZn/Pt and C@FeZn/Ru electrodes were determined as −1.491, −1.490, −1.466 and −1.442 $V_{Ag/AgCl}$ for hydrogen evolution, respectively. C@FeZn/Ru electrode have more positive potential as a comparison with CFeZn, C@FeZn, and C@FeZn/Pt electrodes for HER. It is explained that CFeZn/Ru electrode has the lowest hydrogen evolution overpotential. As it is well-known in the literature, the enhanced catalytic activity of electrodes exceedingly is influenced by its chemical composition, large specific surface area, and nanostructure [30].

The EIS results were obtained for C@FeZn, C@FeZn/Pt, and C@FeZn/Ru electrodes as a cathode material with regards to HER in alkaline solution in the frequency range from 10^6 to 0.01 Hz.

The inhomogeneities of coating surface cause the deviation from the ideal semicircle of Nyquist plot. All of the electrodes have two loops. It was a large depressed capacitive loop and an inductive loop at the high-frequency region and the low-frequency region, respectively. The capacitive loop is related to the charge transfer resistance. Linear portion related to hydrogen evolution reaction is diffusion controlled [14]. It is seen from Fig. 3, the Nyquist plot of C@FeZn/Ru has the smallest capacitive loop. Also, the inductive loop has the smaller angle than others. It is understood that C@FeZn/Ru has the lowest catalyst resistance and diffusion rate in comparison with C@FeZn and C@FeZn/Pt which indicate that it was more active from other electrodes for HER.

The equivalent circuit was used for illustrating the electrode/solution interface in Fig. 4. The elements of the circuit can be named as; R_s is the solution resistance, R_{ct} is the charge transfer resistance, R_d is the diffuse layer resistance which corresponds to the resistance of all accumulated species [31], and CPE_{dl} is the constant phase element namely, the capacitance of the double layer. Total polarization resistance (R_p) of the electrode must be equal to the sum of R_{ct} and R_d. R_f and CPE_f reflect the film resistance coating metals and capacitance of the film layer [34], respectively. Here, total R_p value includes the film resistance and it is equal to the sum of R_{ct}, R_d and R_f values ($R_p = R_{ct} + R_d + R_f$).

A satisfactory fitting was achieved to represent depressed semi-circles by replacing C with CPE in the equivalent circuit. The impedance of the CPE is given as [31]:

$$Z_{CPE} = \frac{1}{Y_0(J \times W^n)} \quad (1)$$

the elements of the equation can be defined as Y_0 is the magnitude of the CPE, n is the phase shift which indicates that the deposited coatings had a porous structure when it was lower than 1.0, j is the imaginary unit, and W is the angular frequency.

The increasing surface area was positively affected the catalytic efficiency of electrodes via decreasing the resistance of R_p in Nyquist plots. The low amount loading of noble metal on C@FeZn electrodes decrease the R_p values. R_s, $R_{ct} + R_d$ and CPE_{dl} are independent of potential change at the high-frequency level, and it is dependent to surface porosity, but R_f and CPE_f are related to potential at low-frequency level due to Faradaic process of HER [32]. The decreasing of the angle of a linear portion at low-frequency region showed that the HER was eased.

The obtained results explain the enhancement of HER activity of electrodes after low metal loading. C@FeZn/Ru catalyst displays the lowest R_p value (Table 2).

Analyzes of potentiodynamic polarization curves were detected at 1 mV s^{-1} scan rate in 1.0 M KOH solution in Fig. 5. Overpotential is one of the most practical methods for catalytic effect of the electrode in HER at a given current density, in our studies at 10, 50 and 100 mA cm^2 ($-\eta_{10}$, $-\eta_{50}$, $-\eta_{100}$). The overpotential is directly related to the catalytic efficiency of electrodes. Increasing overpotentials cause the decreasing of current density [17]. Therefore, it is important to follow the changes while comparing of electrode activity. Having lower overpotential as the same current density within the various electrode materials shows higher catalytic activity for the HER.

As seen in Fig. 5, C@FeZn/Pt and C@FeZn/Ru catalysts exhibit lower overpotentials for $-\eta_{50}$ values, −80 mV and −30 mV, compared to C@FeZn. C@FeZn/Ru have the lowest overpotential for each $-_{\eta}$ values. It is explained that the C@FeZn/Ru electrode has the most catalytic efficiency. The parameters attained by the potentiodynamic polarization analysis in Fig. 5 are listed in Table 3.

The dissociative adsorption of water molecules plays a key role in the mechanism and kinetic of hydrogen discharged from the alkaline solution, and the generally accepted mechanism of hydrogen evolution in alkaline solution is performed by Volmer reaction (2) [4]. After this step followed by either Heyrovsky reaction (3) (electrochemical desorption), or Tafel reaction (4) (chemical recombination) [33].

$$H_2O + M + e^- \rightleftharpoons MH_{ads} + OH^- \quad \text{(Volmer)} \tag{2}$$

$$H_2O + MH_{ads} + e^- \rightleftharpoons H_2 + M + OH^- \quad \text{(Heyrovsky)} \tag{3}$$

$$MH_{ads} + MH_{ads} + e^- \rightleftharpoons H_2 + 2M \quad \text{(Tafel)} \tag{4}$$

Here M and MHads are the active sites and hydrogen atom adsorbed on the metal surface, respectively. When the Tafel slope should yield about 120 mV dec^{-1} at 30 °C, primary rate determining step (rds) for HER are determined as Volmer reaction step, i.e. adsorption of hydrogen, according to the general model for the HER mechanism in alkaline media [30,34]. When the Tafel slope is 40 mV dec^{-1} for Heyrovsky reaction as the rds or 30 mV dec^{-1} the rds is the Tafel reaction [35].

It could also be realized that the measured Tafel slope values slightly increase from the 120 mV dec^{-1}. This phenomenon has already been reported in the literature [35–37], Fe is covered by a thin layer of Fe-oxide. Hence, the presence of thin oxide film on the surface could be related to the deviated Tafel slope values. Since Fe-oxide act as a semiconductor. The electronic conductivity of Fe-oxide is lower than the conductivity of metallic Fe. This results in a decrease in symmetry factor, β, and an increase in Tafel slope, given the fact that the reaction mechanism does not change. Note that for the Volmer step as the rds, the symmetry factor, β, is equal to the transfer coefficient, α, while for the Heyrovsky step as the rds, the transfer coefficient is $\alpha = 1+\beta$ [35].

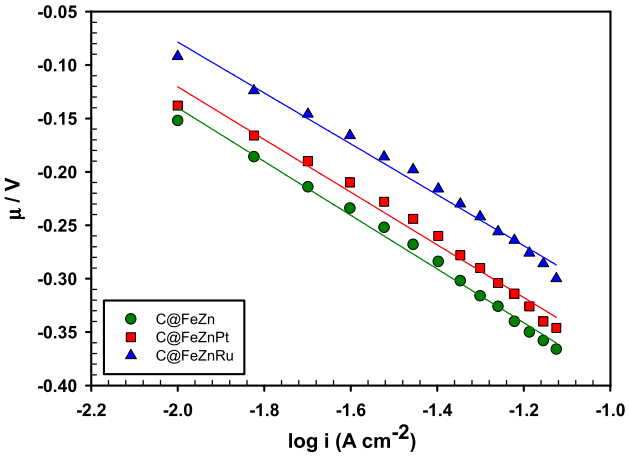

Fig. 5 – The cathodic potentiodynamic polarization curves of C@FeZn, C@FeZn/Pt and C@FeZn/Ru electrodes in 1.0 M KOH.

$$\mu = a + b\,logi \tag{5}$$

where μ (V) represents the applied overpotential, a (V) and b (V dec^{-1}) are the Tafel constants, and i is the current density (A cm^{-2}).

$$\log(i_0) = -\frac{a}{b} \tag{6}$$

$$\alpha = \frac{2.303 \times R \times T}{b \times n \times F} \tag{7}$$

Here R is (8.314 J mol^{-1} K^{-1}) is gas constant, represents the number of electrons exchanged, T is the thermodynamic temperature (K), and F (96,487 C mol^{-1}) is Faraday constant.

The thin oxide layer formed on the Fe surface overcome a low electron transfer barrier located inside the thin oxide film (band gap). This gives a lower transfer coefficient value, $\alpha Fe = \beta Fe = 0.257$.

The Tafel plots for all binary and ternary cathode are linear at negative potentials. This is indicating that the predominant mechanism of HER on these electrodes appears to be a discharge of water (Volmer reaction) followed by electrochemical desorption step (Heyrovsky). The highest b value was determined for the C@FeZn electrode. The highest value specifies the worst electrocatalytic properties for HER [32].

Table 2 – Calculated fitting parameters from EIS data in 1.0 M KOH solution.

	R1	R2	Y_0*10^{-4}	n1	R3	Y_0*10^{-4}	n2	W
C@FeZn	1.302	1.525	309.1	0.541	30.0	7629	0.61	−40.48
C@FeZn/Pt	1.232	2.263	352.4	0.725	16.6	8253	0.76	28.48
C@FeZn/Ru	1.301	0.849	360.1	0.776	7.5	9779	0.97	1.35

Table 3 – The electrochemical data determined from cathodic potentiodynamic polarization curves at different overpotentials.

	$-\eta_{10}$ (V)	$-\eta_{50}$ (V)	$-\eta_{100}$ (V)	i_0 (mA cm^{-2})	b (mV dec^{-1})	α
C@FeZn	0.150	0.320	0.381	2.951	252	0.242
C@FeZn/Pt	0.138	0.290	0.368	3.310	247	0.247
C@FeZn/Ru	0.090	0.242	0.348	4.681	238	0.257

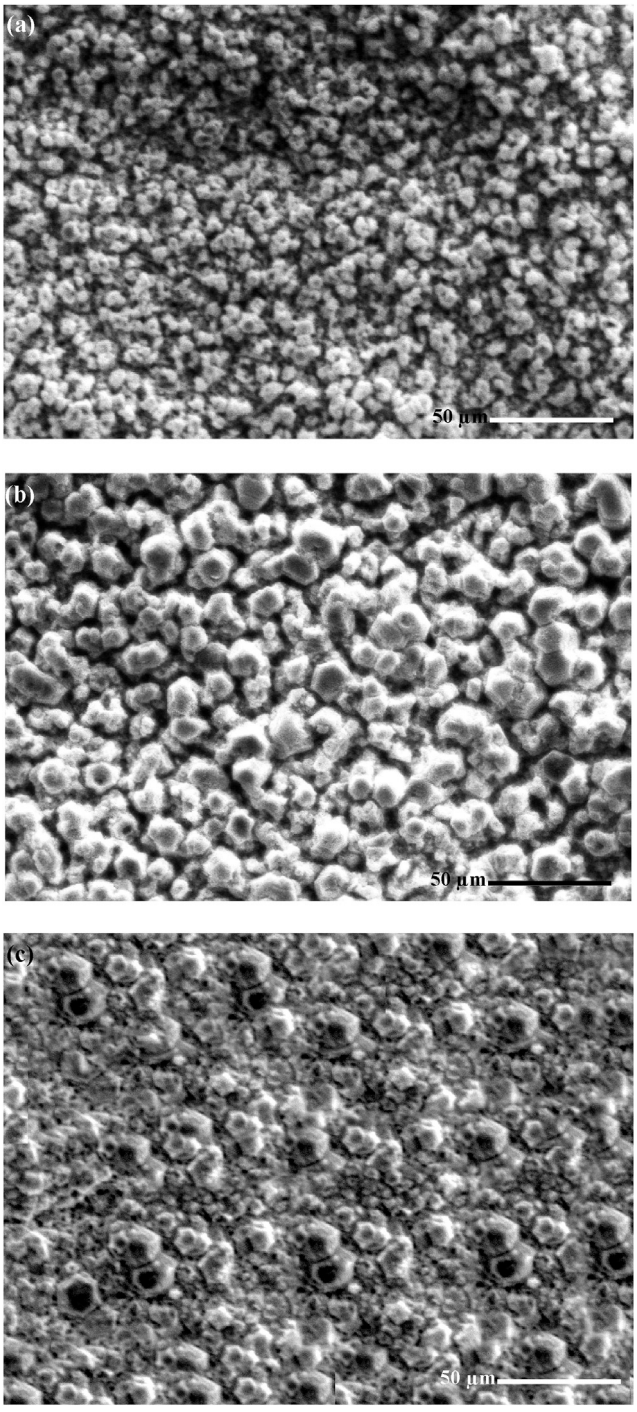

Fig. 6 – SEM images of C@FeZn (a), C@FeZn/Pt (b) and C@FeZn/Ru (c) electrodes (mag: 500×).

The large surface area for various electrode materials positively affects the possible mechanism of HER. The leaching of Zn on electrode surface provides a big surface as a cauliflower structure compares with the old version. Also, it is well known the good electrocatalytic fundamental activity of platinum group metals (Pt, Ru, Pd, Rh, Ir) [30,38,39].

As seen in Fig. 6a, the surface of the C@FeZn electrode had cauliflower structure. This structure was closed by Pt, which had a hexagonal structure (Fig. 6b). When Ru was deposited on C@FeZn, cauliflower was seen on the surface together hexagonal Ru (Fig. 6c). Deposition of metallic Pt and Ru particles were changed the surface morphology of C@FeZn electrode. All SEM images were obtained under the same conditions (magnitude: 500× and 50 μm). The chemical compositions of prepared electrodes were determined by EDX. The compositions were given in Table 4.

The system set up with a burette, two electrodes and KOH solution for the hydrogen evolution measurement. A burette was filled with 1.0 M KOH solution and dipped in a beaker was including 1.0 M KOH solution. Preparing electrodes, which was used as the cathode, coiled up under the burette's open side in the electrolyte. The platinum sheet was used as counter electrode. The initial volume was recorded and 30 mA cm^{-2} constant current density was applied to electrodes during 1 h, and the volume of hydrogen gas evolution was monitored by the volume change from the level of the solution at room temperature. In these conditions, the total of hydrogen gas and water vapor measured in the burette as total volume. The hydrogen volumes were calculated with considerations water vapor correction [30]. The measured volumes of hydrogen are given in Table 5. As it can be seen in Table 5, the C@FeZn/Ru catalysts produced more hydrogen gas than other electrodes. Hydrogen ions adsorbed onto the noble metal coated

Table 4 – The chemical compositions of prepared electrodes.

	%Fe	%Zn	%Pt	%Ru
C@FeZn	3.9	96.1	–	–
C@FeZn/Pt	2.3	95.8	1.9	–
C@FeZn/Ru	1.5	96.9	–	1.6

Table 5 – Hydrogen gas volumes produced on preparing electrodes by electrolysis technique applying 30 mA cm^{-2} constant current density over 1 h.

Cathode	V_{H_2} (mL cm^{-2})
C@FeZn	54.8
C@FeZn/Pt	68.5
C@FeZn/Ru	85.6

electrodes, and hydrogen evolution may continue to electrochemical reactions using more active area. The volume of hydrogen gas increases at the C@FeZn/Ru coating.

This study shows that Ru loading on iron–zinc alloy is more efficiently in comparison with Pt loading. It was clarified in the literature by Berry et al. [40] that the s-electron density increases with decreasing d-electron population at the iron nucleus due to Ru loading on the iron surface. Given that ruthenium induces the reduction of iron(m) to iron(II) it is likely that the iron(II) species so formed are near the ruthenium species and that their interaction with ruthenium involves the transfer of d-electrons from the iron(II) to the ruthenium. In this respect, it is interested in the enhanced catalytic activity.

Conclusion

The C@FeZn, C@FeZn/Pt, and C@FeZn/Ru electrodes were prepared and tested for potential use as the cathode catalyst for hydrogen evolution reaction. All of the prepared electrodes were characterized using cyclic voltammetry, electrochemical impedance spectroscopy, and potentiodynamic polarization techniques. The alkaline leaching process can considerably increase the hydrogen evolution activity of the electrode. The results show that the C@FeZn/Ru electrodes are more efficient for hydrogen production by comparison with C@FeZn, C@FeZn/Pt electrodes. The highest hydrogen volume was obtained at C@FeZn/Ru electrode when 30 mA cm^{-2} constant current density was applied to the electrolysis system during 1 h. From the data obtained, the C@FeZn/Ru electrode could be preferred for using hydrogen production.

REFERENCES

[1] Carmo M, Fritz DL, Mergel J, Stolten D. A comprehensive review on PEM water electrolysis. Int J Hydrogen Energy 2013;38:4901–34.

[2] Dincer I, Acar C. Review and evaluation of hydrogen production methods for better sustainability. Int J Hydrogen Energy 2015;40:11094–111.

[3] Gahleitner G. Hydrogen from renewable electricity: an international review of power-to-gas pilot plants for stationary applications. Int J Hydrogen Energy 2013;38:2039–61.

[4] Shibli SMA, Anupama VR, Arun PS, Jineesh P, Suji L. Synthesis and development of nano WO_3 catalyst incorporated Ni–P coating for electrocatalytic hydrogen evolution reaction. Int J Hydrogen Energy 2016;41:10090–102.

[5] Zhao M, Dong H, Chen Z, Ma Z, Wang L, Wang G, et al. Study of Ni–S/CeO_2 composite material for hydrogen evolution reaction in alkaline solution. Int J Hydrogen Energy 2016;41:20485–93.

[6] Danilovic N, Subbaraman R, Strmcnik D, Chang KC, Paulikas A, Stamenkovic V, et al. Enhancing the alkaline hydrogen evolution reaction activity through the bifunctionality of Ni (OH) 2/metal catalysts. Angew Chem 2012;124:12663–6.

[7] Zheng Y, Jiao Y, Zhu Y, Li LH, Han Y, Chen Y, et al. Hydrogen evolution by a metal-free electrocatalyst. Nat Commun 2014;5.

[8] Wang Y, Yang X, Wang Y. Catalytic performance of mesoporous MgO supported Ni catalyst in steam reforming of model compounds of biomass fermentation for hydrogen production. Int J Hydrogen Energy 2016;41:17846–57.

[9] Baslak C, Aslan E, Patir IH, Kus M, Ersoz M. Photocatalytic hydrogen evolution based on mercaptopropionic acid stabilized CdS and CdTeS quantum dots. Int J Hydrogen Energy 2016;41:20523–8.

[10] Dahbi S, Aboutni R, Aziz A, Benazzi N, Elhafyani M, Kassmi K. Optimised hydrogen production by a photovoltaic-electrolysis system DC/DC converter and water flow controller. Int J Hydrogen Energy 2016;41:20858–66.

[11] Safizadeh F, Ghali E, Houlachi G. Electrocatalysis developments for hydrogen evolution reaction in alkaline solutions–A Review. Int J Hydrogen Energy 2015;40:256–74.

[12] Subbaraman R, Tripkovic D, Chang K-C, Strmcnik D, Paulikas AP, Hirunsit P, et al. Trends in activity for the water electrolyser reactions on 3d M (Ni, Co, Fe, Mn) hydr (oxy) oxide catalysts. Nat Mater 2012;11:550–7.

[13] Wang Y, Zhang G, Xu W, Wan P, Lu Z, Li Y, et al. A 3D nanoporous Ni–Mo electrocatalyst with negligible overpotential for alkaline hydrogen evolution. ChemElectroChem 2014;1:1138–44.

[14] Telli E, Döner A, Kardaş G. Electrocatalytic oxidation of methanol on Ru deposited NiZn catalyst at graphite in alkaline medium. Electrochim Acta 2013;107:216–24.

[15] Shibli SMA, Dilimon VS. Development of TiO_2-supported nano-RuO_2-incorporated catalytic nickel coating for hydrogen evolution reaction. Int J Hydrogen Energy 2008;33:1104–11.

[16] Shibli SMA, Sebeelamol JN. Development of Fe_2O_3–TiO_2 mixed oxide incorporated Ni–P coating for electrocatalytic hydrogen evolution reaction. Int J Hydrogen Energy 2013;38:2271–82.

[17] Solmaz R, Kardaş G. Electrochemical deposition and characterization of NiFe coatings as electrocatalytic materials for alkaline water electrolysis. Electrochim Acta 2009;54:3726–34.

[18] Ullal Y, Hegde AC. Electrodeposition and electro-catalytic study of nanocrystalline Ni–Fe alloy. Int J Hydrogen Energy 2014;39:10485–92.

[19] Sequeira CAC, Santos DMF, Brito PSD. Electrocatalytic activity of simple and modified Fe–P electrodeposits for hydrogen evolution from alkaline media. Energy 2011;36:847–53.

[20] Vázquez-Gómez L, Cattarin S, Guerriero P, Musiani M. Preparation and electrochemical characterization of Ni+ RuO 2 composite cathodes of large effective area. Electrochim Acta 2007;52:8055–63.

[21] Ananth MV, Parthasaradhy NV. Hydrogen evolution characteristics of electrodeposited Ni-Zn-Fe coatings in alkaline solutions. Int J Hydrogen Energy 1997;22:747–51.

[22] Hu C-C, Tsay C-H, Bai A. Optimization of the hydrogen evolution activity on zinc–nickel deposits using experimental strategies. Electrochim Acta 2003;48:907–18.

[23] Solmaz R, Döner A, Kardaş G. Electrochemical deposition and characterization of NiCu coatings as cathode materials for hydrogen evolution reaction. Electrochem Commun 2008;10:1909–11.

[24] Song L, Wang X, Wen F, Niu L, Shi X, Yan J. Hydrogen evolution reaction performance of the molybdenum disulfide/nickel–phosphorus composites in alkaline solution. Int J Hydrogen Energy 2016;41:18942–52.

[25] Habibi B, Pournaghi-Azar M, Abdolmohammad-Zadeh H, Razmi H. Electrocatalytic oxidation of methanol on mono and bimetallic composite films: Pt and Pt–M (M = Ru, Ir and Sn) nano-particles in poly (o-aminophenol). Int J Hydrogen Energy 2009;34:2880–92.

[26] Kiani A, Hatami S. Fabrication of platinum coated nanoporous gold film electrode: a nanostructured ultra low-platinum loading electrocatalyst for hydrogen evolution reaction. Int J Hydrogen Energy 2010;35:5202–9.
[27] Paunović P, Radev I, Dimitrov AT, Popovski O, Lefterova E, Slavcheva E, et al. New nano-structured and interactive supported composite electrocatalysts for hydrogen evolution with partially replaced platinum loading. Int J Hydrogen Energy 2009;34:2866–73.
[28] Ramakrishna SUB, Srinivasulu Reddy D, Shiva Kumar S, Himabindu V. Nitrogen doped CNTs supported Palladium electrocatalyst for hydrogen evolution reaction in PEM water electrolyser. Int J Hydrogen Energy 2016;41:20447–54.
[29] Paunović P, Gogovska DS, Popovski O, Stoyanova A, Slavcheva E, Lefterova E, et al. Preparation and characterization of Co–Ru/TiO_2/MWCNTs electrocatalysts in PEM hydrogen electrolyzer. Int J Hydrogen Energy 2011;36:9405–14.
[30] Yüce AO, Döner A, Kardaş G. NiMn composite electrodes as cathode material for hydrogen evolution reaction in alkaline solution. Int J Hydrogen Energy 2013;38:4466–73.
[31] Farsak M, Keleş H, Keleş M. A new corrosion inhibitor for protection of low carbon steel in HCl solution. Corros Sci 2015;98:223–32.
[32] Bachvarov V, Lefterova E, Rashkov R. Electrodeposited NiFeCo and NiFeCoP alloy cathodes for hydrogen evolution reaction in alkaline medium. Int J Hydrogen Energy 10 August 2016;41(30):12762–71.
[33] Herraiz-Cardona I, Ortega E, Vázquez-Gómez L, Pérez-Herranz V. Double-template fabrication of three-dimensional porous nickel electrodes for hydrogen evolution reaction. Int J Hydrogen Energy 2012;37:2147–56.
[34] Kaninski MPM, Nikolić VM, Potkonjak TN, Simonović BR, Potkonjak NI. Catalytic activity of Pt-based intermetallics for the hydrogen production—influence of ionic activator. Appl Catal A General 2007;321:93–9.
[35] Navarro-Flores E, Chong Z, Omanovic S. Characterization of Ni, NiMo, NiW and NiFe electroactive coatings as electrocatalysts for hydrogen evolution in an acidic medium. J Mol Catal A Chem 2005;226:179–97.
[36] Królikowski A, Wiecko A. Impedance studies of hydrogen evolution on Ni·P alloys. Electrochim Acta 2002;47:2065–9.
[37] Łosiewicz B, Budniok A, Rówiński E, Łągiewka E, Lasia A. The structure, morphology and electrochemical impedance study of the hydrogen evolution reaction on the modified nickel electrodes. Int J Hydrogen Energy 2004;29:145–57.
[38] Barber J, Conway B. Structural specificity of the kinetics of the hydrogen evolution reaction on the low-index surfaces of Pt single-crystal electrodes in 0.5 M dm− 3 NaOH. J Electroanal Chem 1999;461:80–9.
[39] Solmaz R, Gündoğdu A, Döner A, Kardaş G. The Ni-deposited carbon felt as substrate for preparation of Pt-modified electrocatalysts: application for alkaline water electrolysis. Int J Hydrogen Energy 2012;37:8917–22.
[40] Berry FJ, Liwu L, Chengyu W, Renyuan T, Su Z, Dongbai L. An in situ Mössbauer investigation of the influence of metal–support and metal–metal interactions on the activity and selectivity of iron–ruthenium catalysts. J Chem Soc Faraday Trans 1 Phys Chem Condens Phases 1985;81:2293–305.